Electrospinning of Highly Crystalline Polymers for Strongly Oriented Fibers

*Arnaud W. Laramée, Catherine Lanthier and Christian Pellerin**

Département de chimie, Université de Montréal, Montréal, QC, H3C 3J7, Canada

ABSTRACT: Electrospun nanofibers (NFs) often demonstrate an exponential increase in mechanical and other properties at reduced diameters. Molecular orientation emerges as a key parameter for the performance of amorphous and low crystallinity polymers, but single-fiber structural investigations are still lacking for highly crystalline polymers. Herein, polarized confocal Raman spectroscopy reveals that fibers of highly crystalline poly(ethylene oxide) (PEO) maintain a high orientation over a broad range of diameters, in strong contrast with the usual exponential trend. This observation stands for five electrospinning solvents of widely different properties. By comparison, poly(oxymethylene) (POM) NFs also show a high orientation at low diameters but it decreases substantially for diameters larger than ~1400 nm, a result attributed to the lower crystallinity of POM compared to PEO. The results show that the exponential orientation dependence on fiber diameter is not universal and stress the importance of polymer crystallinity on the structure and properties of electrospun nanofibers. This work guides the preparation of fibers with optimal orientation-dependent properties and shows that high crystallinity can afford more robust materials whose performance is less affected by variations in experimental conditions, a valuable feature for most application.

Keywords: Fibers, Electrospinning, Crystallinity, Molecular orientation, Property optimization, Raman spectroscopy.

Introduction

Electrospun nanofibers (NFs) are unidimensional nanostructures formed by the solidification of a thin electrified jet generally drawn from a viscous polymer solution.[1-8] Their nanoscale diameter, continuous structure, and relative ease of preparation make them valuable materials for applications such as sensing, electronics, filtration, tissue engineering, drug delivery, as well as energy harvesting, conversion and storage.[8-9] Notably, electrospun NFs attract much attention thanks to their remarkable mechanical, thermal, and electrical properties, which partially stem from molecular anisotropy induced by the strong elongational forces acting on the polymer chains during fiber formation.[1, 8, 10] Experimental[10-20] and theoretical[21-26] works indicate that these properties and the molecular organization from which they appear to originate, strongly depend on fiber diameter. Accordingly, it is crucial to unravel their interplay for the optimization and broader use of these promising nanomaterials.[10-13]

The distinct mechanical properties of NFs, compared to those in the bulk state, were first examined by tensile testing experiments conducted on mats of fibers prepared from polymers of various crystallinities.[27-29] Measurements on mats partly reflect on the intrinsic properties of the individual NFs but they also depend, on a larger scale, on the presence of binding sites between the fibers, the porosity of the mat, and the macroscopic fiber alignment.[28-29] Studies at the single fiber level provide more direct insight and have revealed an exponential increase in Young modulus with a reduction of diameter for NFs of amorphous,[13, 17, 20, 26] moderately crystalline,[15-

[16, 22, 30] and highly crystalline[27, 31-32] polymers. This unique behavior has proven to extend to other mechanical properties and, in some cases, to the highly desirable simultaneous increase in strength and toughness.[10, 13, 16] The most outstanding increase in modulus was reported for NFs of highly crystalline polyethylene (PE),[27, 31] where a ~50-fold increase was found for the thinnest compared to the largest fibers. The onset diameter at which property enhancement occurs varies greatly from one system to another, ranging from ~200 nm[15-16, 22] to up to several micrometers[17, 20] when the molecular weight of the polymer is unusually high.[20] Interestingly, electrical and thermal properties such as piezoelectricity,[33] electrical conductivity,[34] and thermal conductivity[35] were also shown to follow a similar trend for specific systems. Other physical properties such as the glass transition temperature (T_g) and melting temperature are also impacted by the fiber diameter but conflicting trends have been reported.[17-19, 36-37]

The intriguing properties observed in single-fiber studies prompt the investigation of the underlying structural origin for further optimization. Theoretical models suggest that molecular ordering induced by the elongational forces during the electrospinning process is a key element of the structure-property relationships.[20-25] In particular, Greenfeld et al. proposed that the exponential increase in modulus, strength and toughness observed experimentally for NFs below the onset diameter is caused by a transition between the coil and stretch chain extension states at a critical diameter value, d_c, when the extensional flow reaches sufficiently high deformation rates.[21] Experimental studies at the mat level by infrared (IR) spectroscopy and X-ray diffraction (XRD) support the important role of molecular orientation in explaining NFs' properties.[25, 29, 37] Such studies also underscore that the highest levels of orientation are observed for highly crystalline materials.[38-41] It is nevertheless difficult to draw unequivocal conclusions because

results are affected by the macroscopic alignment of the fibers in the mat, their diameter polydispersity, and the presence of various types of defects.[1, 10]

Structural studies at the single fiber level are thus required but they remain challenging to conduct. Techniques combining IR spectroscopy and atomic force microscopy enable to distinguish crystal polymorphs within single fibers[42-43] and begin to offer useful insight on their molecular orientation[44-45]. Selected area electron diffraction (SAED) provides quantitative information on crystalline phases and showed a notable increase in orientation in highly crystalline polyethylene NFs with a reduction in diameter.[46] However, only limited information is currently available[46-48] because SAED requires tedious sample preparation that prevents collection of large amounts of data.[1, 10] Polarized Raman microscopy has emerged as a particularly useful characterization method because it allows quantification of molecular orientation in individual NFs of various crystallinities.[1, 10-11, 14, 49-51] Using this method, our group has shown that molecular orientation in amorphous PS fibers, although remaining moderate, follows an exponential-like increase below an onset diameter that is analogous to the previously reported trend for their modulus.[11, 20, 31] Papkov et al. have evaluated molecular orientation in moderately crystalline polyacrylonitrile NFs.[14] Interestingly, they found that large fibers maintain a certain degree of molecular orientation, in contrast to their amorphous counterpart, which can be explained by the crystallites hindering chain mobility and preventing further orientation relaxation once the fibers are deposited on the collector.[14] We recently showed by polarized Raman microscopy that highly crystalline poly(ethylene oxide) (PEO) NFs present a high level of molecular orientation regardless of the collection method, a result that was masked in XRD measurements at the mat level, but the dependence on fiber diameter was not investigated.[52] These results suggest that the degree of crystallinity affects the dependence of

orientation on diameter, and emphasize the need for comprehensive studies of molecular orientation in highly crystalline systems typically associated with sought-after mechanical properties.[27, 31]

In this paper, we use confocal Raman spectroscopy to establish the quantitative relation between molecular orientation and fiber diameter in electrospun fibers of two highly crystalline polymers: PEO and poly(oxymethylene) (POM). Our results indicate that the degree of crystallinity is a critical factor that affects the shape of the diameter dependence of orientation and that can be harnessed to control and uniformize the structural characteristics of electrospun fibers.

Experimental Section

Electrospinning

Poly(ethylene oxide) with a weight-average molecular weight of 400 kg/mol and poly(oxymethylene) (POM) (Scientific Polymer Products, Cat# 136e and 009, respectively) were used as received. Chloroform, N,N-dimethylformamide (DMF), 1,1,1,3,3,3-hexafluoro-2-propanol (HFIP), methanol and distilled water were used as solvents without further purification. Information on their vapor pressure, boiling point and dielectric constant values is provided in Table S1. PEO fibers with a targeted range of diameters were prepared by dissolving an appropriate mass of PEO in 5 ml of solvent to afford 2.5 % and 3.5 % solutions in chloroform, 5.0 % and 7.0 % solutions in HFIP and methanol, and 7.0 % and 9.0 % solutions in DMF and water (m/v). POM fibers with a comparable diameter range were obtained by preparing 5.0 % and 7.0 % solutions of POM in HFIP (m/v) under mild heating (50 ºC). Once the polymer was completely dissolved, the cooled solution was introduced in a 5 mL glass syringe fitted with a

0.41 mm diameter flat-end needle, on which a 15 kV voltage was applied using a CZE 1000R high-voltage power supply (Spellman High Voltage Electronics). A PHD 2000 syringe pump (Harvard Apparatus) was used to secure the syringe and to impose a constant flow generally fixed at 0.03 mL/min, with lower flow values selected for polymer solutions of higher viscosity. The fibers were spun in a fume hood at low relative humidity (typically below 35 %) and at temperatures between 20 and 24 °C. They were collected on a gap collector with a 20 mm separation between the metallic rods on which a negative 2 kV potential was exerted using a Power Designs source. The distance between the needle tip and the collector was fixed at 15 cm. The collection time was adjusted to yield samples of low fiber density for the Raman experiments and mats of higher fiber density for the other characterization techniques. The deposited fibers were carefully transferred onto a microscope slide and dried under vacuum for at least 36 h prior to analysis to minimize traces of residual solvent.

Confocal Raman spectroscopy

Spectra were recorded in the backscattering geometry using the 632.8 nm He-Ne laser of a LabRam HR800 spectrometer (Horiba Scientific) coupled with an Olympus BX41 microscope equipped with a long working distance 100X objective (NA = 0.8). The confocal hole and the slit were set to 100 and 150 μm, respectively. The polarization of the incident laser beam and the of Raman scattered light was set parallel (Z) or perpendicular (X) to the fiber axis using a half-wave plate and an analyzer, respectively. A 600 grooves/mm holographic grating was used in conjunction with a scrambler to minimize the polarization dependence of its diffraction efficiency. The integration time was set between 12 s and 15 s and averaged 12 times for each spectrum. Prior to Raman characterization, small quantities of fibers were cut from the surface of microscope slide with a scalpel, and then transferred and immobilized onto BaF_2 windows with

fine tweezers and adhesive tape. For orientation quantification at the single-fiber level, complete sets of parallel- and cross-polarized spectra were collected, in the order ZZ, ZX, XX, XZ, ZZ(2), on well-isolated individual fibers aligned with their main axis along the Z direction. The second ZZ spectrum was recorded to detect potential drifts or loss of focus during acquisition. Any set of spectra was rejected when the intensity of the band used for orientation quantification differed by more than 5% in the ZZ and ZZ(2) spectra. The orientation parameter $\langle P_2 \rangle$ was calculated using the most probable distribution (MPD) method described in detail in our previous works.[50-52] The $\langle P_2 \rangle$ parameter takes a value of 0 for a completely isotropic system and a maximum value of 1 for perfect orientation of the chains along the fiber axis.

The diameter of each fiber was estimated individually using confocal Raman spectroscopy. In short, a series of 12-15 ZZ spectra was collected at regularly spaced locations perpendicular to the fiber axis (along the X axis on the inset of Figure 1). The signal intensity was then plotted as a function of position, resulting in a gaussian-like curve with a maximum intensity at the center of the fiber. The data was fitted with a gaussian function using Origin 2020b and the fiber diameter taken as the double of the computed standard deviation (σ).

Infrared spectroscopy

Infrared spectra of the POM nanofibers were recorded using a Tensor 27 FT-IR spectrometer (Bruker Optics) with a liquid nitrogen-cooled HgCdTe detector and a MIRacle silicon attenuated total reflection accessory (Pike Technologies). Spectra with a 4 cm^{-1} resolution were obtained by averaging 300 scans. Prior to data collection, densely packed fiber mats were thoroughly ground in order to eliminate anisotropy that could overshadow the morphological information.

Scanning electron microscopy

Field-emission scanning electron microscopy (SEM) images were collected with either Hitachi

Regulus 8230 or JEOL JSM-7400F instruments operated under a high vacuum at voltages between 1.0 and 1.5 kV and a current of 20 μA. No metal coating was deposited onto the nanofiber mats prior to imaging.

Differential scanning calorimetry

Thermal properties were investigated on compacted nanofiber mats weighing between 3.5 and 4.0 mg by differential scanning calorimetry (DSC) with a TA Instruments Q2000 calorimeter calibrated with indium at a heating rate of 10 °C/min. The melting temperature (T_m) and crystallinity index (X) were determined with an initial cycle of heating from -85 °C to 105 °C (PEO) or 205 °C (POM). After cooling (30 °C/min), a second heating scan was performed under the same conditions to collect thermal information on the bulk materials. The enthalpy of fusion of 100 % crystalline PEO and POM used to calculate X were set at 203 and 318 J/g, respectively.[53-54]

Results and Discussion

Poly(ethylene oxide) nanofibers

PEO is a highly crystalline polymer with an excellent solubility in a broad range of solvents. It is commonly used in electrospun NFs, either on its own or as a matrix for other compounds of interest, thanks to its biocompatibility and its high electrospinnability.[9, 55] PEO is therefore a good model system to investigate the incidence of fiber diameter on the molecular orientation of NFs of highly crystalline polymers and the impact of solvent properties. Figure 1 shows a set of four polarized Raman spectra collected from an individual PEO fiber with a 1200 nm diameter. The intensity contrast between the ZZ and XX polarized spectra (a larger spectral range is shown in Figure S1 of the supporting information) reflects the strong preferential orientation of the PEO

chains along the fiber axis (Z direction). The 1072 cm^{-1} band, associated with CH_2 rocking and COC symmetric stretching for trans-gauche-trans conformations,[56] and the 1126 cm^{-1} band, associated with COC symmetric stretching for trans-gauche-trans and trans-trans-trans conformations,[56] are both well-suited for orientation studies. While both bands give similar results, the 1126 cm^{-1} band was preferred because it is better isolated and its intensity can be measured more confidently under all four polarization combinations for NFs covering a wide range of diameters. Its weak intensity in the XX spectrum indicates that the tilt angle of its Raman tensor is close to 0°, thereby allowing to use the calculated order parameter ($\langle P_2 \rangle$) values as a quantitative indicator of the orientation of the polymer backbone with respect to the fiber axis. The acquisition method is robust, with minimal signal drift during the sequence of measuring 5 polarized spectra at the same spot for each fiber, and it enables quantifying molecular orientation in electrospun fibers of diameters ranging from ~600 nm to several micrometers with a rejection rate lower than 10 %.

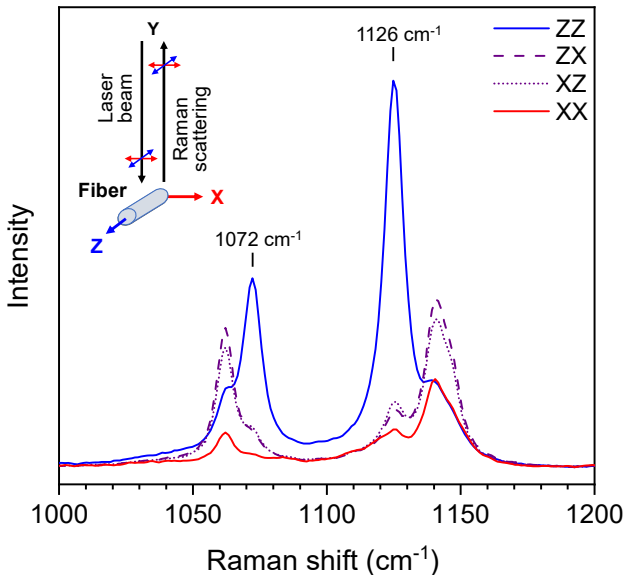

Figure 1. Set of four polarized Raman spectra collected from a PEO fiber with a $\langle P_2 \rangle$ of 0.60 and a diameter of 1200 nm. Inset: Scheme of a polarized confocal Raman spectroscopy experiment for quantification of molecular orientation in an individual fiber. The polarization of the incident laser beam and the scattered light propagating in the Y direction is set parallel (Z) or perpendicular (X) to the fiber axis.

Figure 2 shows the effect of fiber diameter on the molecular orientation of a large quantity of individually interrogated PEO NFs spun using five different solvents. Two main observations stand out. First, the chain orientation is high and is maintained throughout the diameter range accessible, with $\langle P_2 \rangle$ values approximately centered at 0.6 and reaching values up to 0.78 for the smallest diameters. Second, this trend is preserved for fibers prepared using solvents covering a wide range of volatilities and dielectric constants (vide infra). Such high orientation is in good agreement with the previously reported data for PEO and PEO-containing NFs,[38-40, 52] although the electrospinning conditions and resulting diameter range were different. The results sharply contrast with the tendencies reported for amorphous and weakly crystalline NFs, where significant molecular orientation was only observed below a specific onset diameter.[11, 14] PEO NFs rather show a relatively smooth decrease of orientation with diameter (see the inset of Fig.

2) with $\langle P_2 \rangle$ values remaining above 0.5 even for the thickest fibers of ~2.5 µm diameter (fibers prepared in DMF are the only exception with $\langle P_2 \rangle > 0.42$). As discussed below, this contrasting behavior appears to originate from the high crystallinity of PEO,[57] which would shift the onset value to several micrometers, beyond the largest fibers reached here.

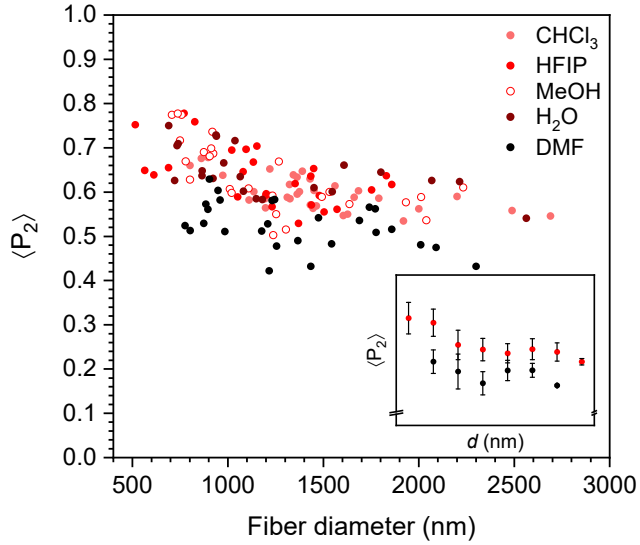

Figure 2. Diameter dependence of molecular orientation for PEO fibers electrospun using various solvents. The color gradient represents qualitatively the solvent volatility, with lighter symbols referring to higher volatility. The inset highlights the lower orientation for fibers spun from DMF (black) compared the other solvents (red).

During the electrospinning process, the strong elongational forces responsible for chain extension compete with chain relaxation processes, leading to a transient orientation that, according to some theoretical models, can be very high in the electrified jet.[4-7] Once the NFs reach the collector, the elongational forces are no longer active but chain relaxation can still occur in the amorphous phase, in particular for polymers with a low T_g or in the presence of residual solvent acting as a plasticizer. This relaxation contributes to the low molecular orientation observed for NFs made of amorphous or weakly crystalline polymers. Larger fibers

are inherently subjected to lower stretching forces while being formed and have a greater tendency to retain solvent due to their lower surface to volume ratio. Both effects lower the final degree of molecular orientation and contribute to the commonly observed exponential decrease in orientation toward a $\langle P_2 \rangle$ value of zero (and to bulk-like properties) for fiber diameters larger than the onset value. In this context, the high $\langle P_2 \rangle$ values and the slow monotonous decreasing trend observed in Figure 2 support that the rapid crystalline growth of oriented nuclei at the stage where chain extension dominates in the electrified jet leads to high orientation.[4, 58] The resulting crystallites then act as physical crosslinking points that prevent chain relaxation despite the T_g of PEO being well below room temperature (a weak T_g was found around -55 °C) .

PEO fibers were spun from solutions in a series of good solvents, $CHCl_3$, HFIP, MeOH, H_2O, and DMF, to establish how their orientation can be controlled by the experimental conditions. Figure 2 shows that the $\langle P_2 \rangle$ values, at any given diameter, are almost identical for NFs spun from this series of solvents of progressively lower volatility (Table S1 provides vapor pressure, boiling point and dielectric constant values), except for fibers drawn from DMF which are slightly less oriented. This behavior was unexpected as both experimental[3, 11, 14] and theoretical[23, 59] studies indicate that the properties of the solvent can affect the level of molecular orientation. A low solvent volatility reduces the evaporation rate and thus contributes to retarding the crystallization process. This favors greater chain relaxation and the formation of randomly oriented crystallites once the fibers are deposited, which can explain the lower orientation of DMF-spun fibers compared to those from the group volatile solvents ($CHCl_3$, HFIP, MeOH). Yet, it does not explain why NFs drawn from H_2O have $\langle P_2 \rangle$ values analogous to those of fibers prepared with these higher volatility solvents. Thus, the influence of the solvent can be better explained by also taking into account its polarity.

In the context of electrospinning, there is strong evidence that the dielectric constant of the solvent affects the trajectory and stability of the electrified jet.[2, 60] More specifically, a solvent with a high dielectric constant, such as H_2O ($\varepsilon = 80.1$),[61] promotes the formation of charges in the jet which increase the electrostatic surface forces responsible for the initiation of bending instabilities.[60] The so-called whipping region of the jet forms when the charge density is either sufficient for the repulsive electrostatic forces to overcome the inertia forces, viscous forces and surface tension, or for a dipolar charge distribution to be initiated in the jet through lateral fluctuations.[2] These instabilities increase the draw ratio, promote higher chain orientation in the jet and lead to thinner fibers.[2, 60] Although counterintuitive, the PEO fibers of a given diameter can thus experience a different draw ratio depending on the solvent used. In fact, the concentration of the PEO solutions had to be varied to achieve equivalent fiber diameters, with solutions in H_2O and DMF (with high ε values) the most concentrated. Therefore, the effect of a higher dielectric constant appears to counteract the effect of a decreased solvent volatility, leading to similar molecular orientation values in Figure 2 and to a similar fiber morphology (Fig. S2) for all solvents. This would explain the high orientation for NFs spun from H_2O, the solvent with the highest dielectric constant, and the lower orientation for fibers spun from DMF, whose moderate dielectric constant ($\varepsilon = 38.3$) would not compensate for its low volatility (Table S1).

It should be noted that the polymer-solvent interaction parameter (χ) can also impact the molecular organization in electrospun NFs, as phase separation may occur for specific systems and influence the chain relaxation and crystallization processes. The five solvents used in this work readily solubilized PEO and did not trigger large scale phase separation during quiescent evaporation, suggesting that the trends of Figure 2 are not severely influenced by differences in

χ. An analogous observation was made for the POM-HFIP system described in the following section.

Poly(oxymethylene) nanofibers

To further understand the impact of the degree of crystallinity on molecular orientation in electrospun NFs, we investigated fibers of poly(oxymethylene) (POM), a polymer with sought-after mechanical properties such as high stiffness and tensile strength.[36-37] The molecular orientation of individual fibers electrospun from HFIP solutions was quantified using the very strong 921 cm^{-1} Raman band associated with COC symmetric stretching[62] (see Fig. S3 for a representative set of four polarized Raman spectra). Similar to the 1126 cm^{-1} band used above for PEO NFs, the 921 cm^{-1} band of POM has a Raman tensor with a tilt angle close to 0°.

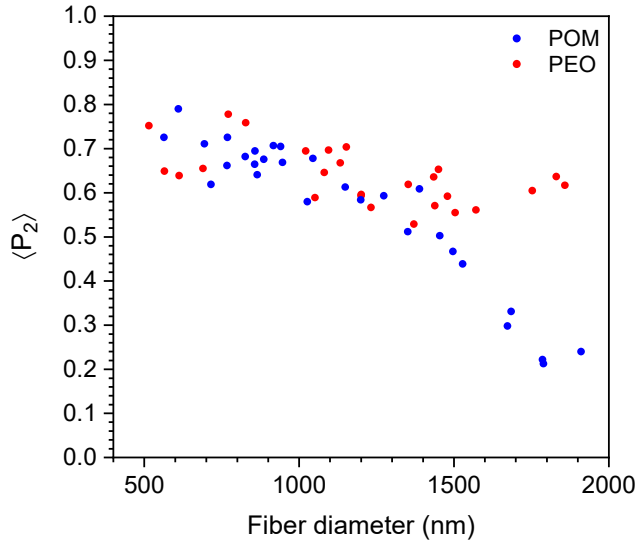

Figure 3. Comparison of the diameter-dependence of molecular orientation in individual fibers of POM and PEO electrospun using HFIP.

Figure 3 compares the molecular orientation in POM and PEO fibers electrospun from solutions in HFIP over a common diameter range. Two regions with contrasting features stand

out. At small diameters, the POM fibers show a high orientation that overlaps with the results obtained with PEO. At diameters larger than 1400 nm, the molecular orientation in POM NFs decreases more abruptly and falls well below that in PEO NFs. This behavior both supports and tempers the conclusion that fibers made of polymers that typically present a high degree of crystallinity (confirmed below by DSC for PEO and POM fibers) maintain a high molecular orientation over an extended range of diameters and do not show the typical exponential trend below a certain onset diameter.

POM and PEO are both polymers with a low T_g that should promote chain relaxation in the absence of crystallites. While a clear T_g could not be detected by DSC for the POM fibers, its reported value[63] of ca. -50 °C is almost identical to that measured for PEO. This suggests that a difference in T_g does not explain their distinct orientation-diameter trends. Another possible origin is the existence of two morphologies associated with the thermodynamically stable trigonal crystalline phase of POM, namely folded-chain crystals (FCC) and extended-chain crystals (ECC), whose prevalence depends on mechanical and thermal conditions under which crystallization occurs.[37, 64] Kongkhlang et al. suggested, on the basis of IR observations, that the large elongational forces involved in the electrospinning process combined with further stretching during the collection step could induce the ECC morphology in POM NFs.[37] The abrupt variation in molecular orientation observed in Figure 3 for d > 1400 nm could thus be caused by a transition from a predominantly ECC morphology to a predominantly FCC one. However, the Raman spectra of fibers at the extremes of the diameter range do not show the 897 cm^{-1} and 1009 cm^{-1} bands reported to be characteristic of the ECC morphology (Fig. S4).[65] Similarly, the spectra do not show the 909 cm^{-1} band associated with the metastable orthorhombic crystalline form.[64]

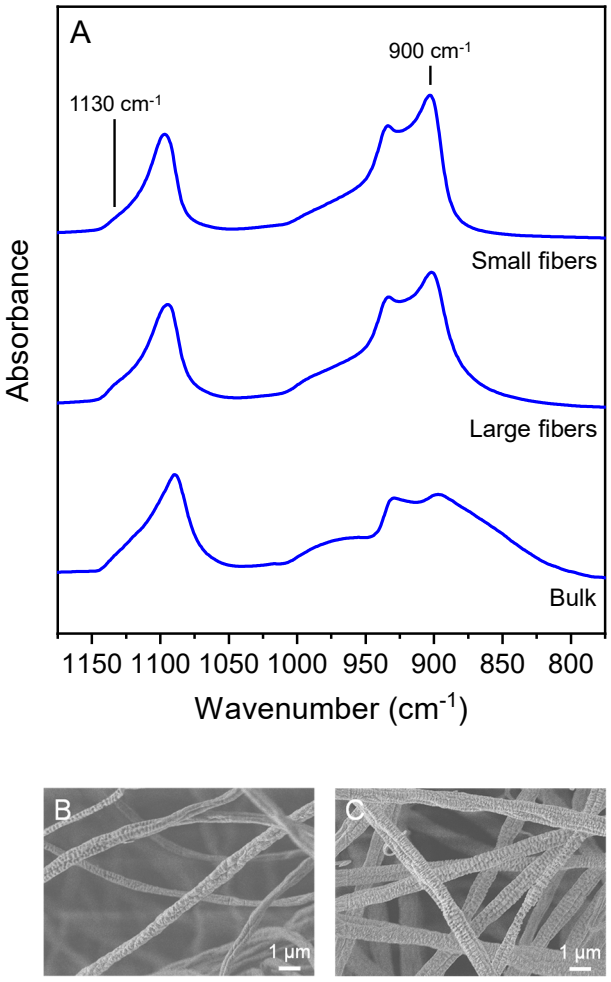

Figure 4. A) IR spectra collected from isotropized POM samples comprised of small NFs, large NFs, and bulk material; B-C) SEM pictures showing the topology of smaller (B) and larger (C) fibers.

IR spectroscopy is seemingly more sensitive to the crystal morphology of POM than Raman spectroscopy,[37, 65] while X-ray diffraction patterns are invariant in this context[66]. Figure 4A shows IR spectra collected on two isotropized mats of fibers spun from solutions of 5.0 % and 7.0 % POM concentration that provides fibers of smaller and larger diameters, respectively. The spectra are similar except for small differences in relative intensity at 900 and 1130 cm^{-1}. The 900 cm^{-1} band, associated with antisymmetric COC stretching and CH_2 rocking, and the 1130

cm^{-1} shoulder, associated with antisymmetric COC stretching and OCO bending,[65] were previously assigned to the ECC and FCC structures, respectively.[37] Larger fibers could thus comprise a somewhat larger FCC fraction that would be consistent with the drop in molecular orientation observed in Figure 3 for $d > 1400$ nm. However, recent works by Nagai et al.[67-68] on the spectroscopic properties of POM question the validity of these assignments. On the basis of comprehensive measurements and calculations, they attributed the broad and highly polarized atypical features observed in the IR spectra of POM (and a few other strongly absorbing polymers) to radiative surface polaritons. These so-called "polariton modes" are mainly observed in spectral regions where the real part of the relative permittivity is negative, which occurs for POM between 900 and 1000 cm^{-1} and around 1110 cm^{-1}. Their intensity, width, and spectral position appear to strongly depend on surface topology, such as the size and shape of pore-like features, rather than on the crystal morphology, making the interpretation of normal modes located in the same spectral regions intricate and potentially misleading.[67-68] SEM images show that POM fibers exhibit surface irregularities that are more pronounced for larger fibers (Fig. 4C) than for smaller fibers (Fig. 4B). Such surface irregularities, which were not observed for the PEO fibers (Fig. S2), recall the porous structures that Nagai et al. have correlated with polaritonic response.[67] Moreover, the large spectral differences between the spectra of fibers and of a bulk POM sample, whose surface characteristics are very different, suggest that the spectral differences between small and large fibers result from the topological dependence of the polariton modes.[37, 67] Accordingly, the decrease in molecular orientation with increasing diameter for POM NFs does not appear to be driven by a diameter-dependent transition in crystal morphology.

Effect of polymer crystallinity on the diameter-dependence of molecular orientation

Our results clearly show that NFs made of highly crystalline polymers exhibit contrasting molecular orientation trends as a function of fiber diameter compared to their amorphous and weakly crystalline counterparts (Figs. 2 and 3). Considering that differences in T_g can be excluded and the lack of experimental evidence for a change in POM crystal morphology, the relative degree of crystallinity of PEO and POM could be the key to their dissimilar orientation at larger fiber diameters. The DSC thermograms of the as-spun NFs shown in Figure 5 reveal a substantial difference in crystallinity between PEO and POM, with PEO fibers reaching X values ~15 % higher than POM fibers spun under analogous conditions. Such difference is consistent with the data obtained from the corresponding bulk materials (Fig. S5). While the crystal growth rate of both polymers is fast and of the same order of magnitude when measured 20 °C below their respective T_m,[69] the crystallization of POM could be kinetically limited during the electrospinning process, once the solvent has mostly evaporated, due to its T_m ~110 ºC higher. These growth rates are up to five orders of magnitude higher than that of weakly crystalline polyacrylonitrile,[70] for which a well-defined exponential-like $\langle P_2 \rangle$ vs. d curve is observed.[3] This reinforces that polymer crystallinity, which in this context closely relates to crystal growth rate due to time constraints, impacts the onset diameter below which a significant increase in molecular orientation occurs.

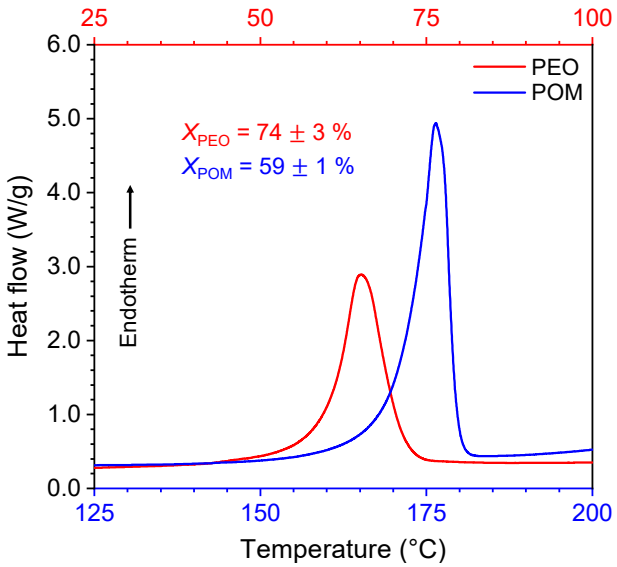

Figure 5. DSC thermograms of the as-spun PEO and POM electrospun fiber mats with the calculated degrees of crystallinity (X_{PEO} and X_{POM}).

Understanding the factors dictating the onset diameter value and the degree of molecular orientation reached is important for various applications because orientation affects several properties of the fibers. A wealth of theoretical models have been developed to rationalize the collective impact of electrospinning parameters (e.g., solution concentration, viscosity, electric conductivity, initial jet velocity, etc.) on molecular orientation and mechanical properties as a function of fiber diameter.[3, 5, 17, 21-22, 59] In particular, Greenfeld et al.[21] have proposed a comprehensive model in which fibers with a diameter d larger than a critical diameter d_c present a mild molecular orientation, whereas the orientation of fibers with $d < d_c$ rapidly increases in an exponential-like manner with a further decrease in d. Most importantly in the context of our results, this model predicts that orientation eventually reaches a plateau at low diameters. Mechanical properties are expected to follow an analogous evolution with the exception that they do not appear to reach a plateau at low diameters.[21] When considering the shape of the $\langle P_2 \rangle$ vs. d curves (Figs. 2 and 3) in view of this model, the high and almost invariant molecular orientation of PEO, throughout the investigated diameter range, reveals that the onset diameter or $d_{c,PEO}$

value is high and beyond those normally reached by electrospinning, even when the onset is shifted to higher values when using polymers of much higher molecular weight. In fact, we previously encountered PEO fibers that retained a high orientation despite having a diameter as large as 10 μm.[52] The d_c value of POM does not fall within the range of diameters considered either. Nevertheless, we note that $d_{c,POM} < d_{c,PEO}$ because of the progressive increase in molecular orientation for d between 2000 and 1400 nm before plateauing at lower d. Following this trend, fibers of low crystallinity or amorphous polymers present the typical exponential-like orientation increase below a well-defined d_c, with $\langle P_2 \rangle$ values tending toward zero above d_c for the latter.[11, 14]

It is worth emphasizing, from an application perspective, that the high level of molecular orientation in fibers of highly crystalline polymers contributes to the optimization of several orientation-dependent physical properties. Furthermore, the fact that this orientation is almost constant, over a vast diameter range and under various spinning conditions, implies that the properties of fibers of highly crystalline polymers are much less affected by the inhomogeneities inherently present in electrospun mats compared to less crystalline systems, leading to more stable and repeatable performance.

Conclusion

This work sheds light on the interrelation between molecular orientation and diameter in electrospun fibers made of highly crystalline polymers. Raman spectroscopy measurements on individual poly(ethylene oxide) (PEO) fibers highlight a large and almost constant orientation throughout a large diameter range (700 – 2700 nm), regardless of the solvent from which they were spun. This sharply contrasts with the exponential increase in orientation (or modulus)

typically observed below a specific onset diameter for electrospun fibers of lower crystallinity or amorphous polymers. This distinct lack of diameter dependence for PEO nanofibers is supported and complemented by measurements on poly(oxymethylene) (POM) fibers. Although PEO and POM show very similar orientations at low diameters, a contrasting trend is observed at larger diameters where the POM orientation decreases abruptly. Infrared spectroscopy and DSC measurements indicate that this discrepancy is best rationalized by the lower degree of crystallinity of POM. This fundamental property appears to play a pivotal role in directing the extent of molecular orientation and its dependence with the diameter of electrospun fibers, including the location of the onset diameter. This new insight can help optimize the mechanical, optical and conduction properties of nanofibers and provides a simple route to produce electrospun materials with more consistent performance.

ASSOCIATED CONTENT

Supporting Information. The following files are available free of charge.

Additional Raman spectra, SEM images and DSC thermograms (PDF)

AUTHOR INFORMATION

Corresponding Author

* Email: c.pellerin@umontreal.ca

Author Contributions

The manuscript was written through contributions of all authors. All authors have given approval to the final version of the manuscript.

Funding Sources

Natural Science and Engineering Research Council of Canada (NSERC) RGPIN-04014-2015.

ACKNOWLEDGMENT

This work was supported by the Natural Science and Engineering Research Council of Canada (NSERC). A.W.L. and C.L. thank the NSERC and Fonds de Recherche du Québec – Nature et Technologies (FRQNT) for graduate scholarships.

REFERENCES

(1) Richard-Lacroix, M.; Pellerin, C. Molecular Orientation in Electrospun Fibers: From Mats to Single Fibers. *Macromolecules* **2013,** *46* (24), 9473-9493.

(2) Reneker, D. H.; Yarin, A. L.; Fong, H.; Koombhongse, S. Bending instability of electrically charged liquid jets of polymer solutions in electrospinning. *J. Appl. Phys.* **2000,** *87* (9), 4531-4547.

(3) Camposeo, A.; Greenfeld, I.; Tantussi, F.; Moffa, M.; Fuso, F.; Allegrini, M.; Zussman, E.; Pisignano, D. Conformational Evolution of Elongated Polymer Solutions Tailors the Polarization of Light-Emission from Organic Nanofibers. *Macromolecules* **2014,** *47* (14), 4704-4710.

(4) Reneker, D. H.; Yarin, A. L. Electrospinning jets and polymer nanofibers. *Polymer* **2008,** *49* (10), 2387-2425.

(5) Greenfeld, I.; Arinstein, A.; Fezzaa, K.; Rafailovich, M. H.; Zussman, E. Polymer dynamics in semidilute solution during electrospinning: a simple model and experimental observations. *Phys. Rev. E Stat. Nonlin. Soft Matter Phys.* **2011,** *84* (4 Pt 1), 041806.

(6) Reneker, D. H.; Yarin, A. L.; Zussman, E.; Xu, H. Electrospinning of Nanofibers from Polymer Solutions and Melts. In *Advances in Applied Mechanics*; Aref, H.; van der Giessen, E., Eds.; Elsevier: 2007; pp 43-346.

(7) Li, X.; Lin, J. Y.; Zeng, Y. C. Electric field distribution and initial jet motion induced by spinneret configuration for molecular orientation in electrospun fibers. *Eur. Polym. J.* **2018,** *98*, 330-336.

(8) Xue, J.; Wu, T.; Dai, Y.; Xia, Y. Electrospinning and Electrospun Nanofibers: Methods, Materials, and Applications. *Chem. Rev.* **2019,** *119* (8), 5298-5415.

(9) Cleeton, C.; Keirouz, A.; Chen, X. F.; Radacsi, N. Electrospun Nanofibers for Drug Delivery and Biosensing. *ACS Biomater. Sci. Eng.* **2019,** *5* (9), 4183-4205.

(10) Papkov, D.; Delpouve, N.; Delbreilh, L.; Araujo, S.; Stockdale, T.; Mamedov, S.; Maleckis, K.; Zou, Y.; Andalib, M. N.; Dargent, E.; Dravid, V. P.; Holt, M. V.; Pellerin, C.; Dzenis, Y. A. Quantifying Polymer Chain Orientation in Strong and Tough Nanofibers with Low Crystallinity: Toward Next Generation Nanostructured Superfibers. *ACS Nano* **2019,** *13* (5), 4893-4927.

(11) Richard-Lacroix, M.; Pellerin, C. Orientation and Partial Disentanglement in Individual Electrospun Fibers: Diameter Dependence and Correlation with Mechanical Properties. *Macromolecules* **2015,** *48* (13), 4511-4519.

(12) Stachewicz, U.; Bailey, R. J.; Wang, W.; Barber, A. H. Size dependent mechanical properties of electrospun polymer fibers from a composite structure. *Polymer* **2012,** *53* (22), 5132-5137.

(13) Pai, C. L.; Boyce, M. C.; Rutledge, G. C. Mechanical properties of individual electrospun PA 6(3)T fibers and their variation with fiber diameter. *Polymer* **2011,** *52* (10), 2295-2301.

(14) Papkov, D.; Pellerin, C.; Dzenis, Y. A. Polarized Raman Analysis of Polymer Chain Orientation in Ultrafine Individual Nanofibers with Variable Low Crystallinity. *Macromolecules* **2018,** *51* (21), 8746-8751.

(15) Tan, E. P. S.; Lim, C. T. Physical properties of a single polymeric nanofiber. *Appl. Phys. Lett.* **2004,** *84* (9), 1603-1605.

(16) Papkov, D.; Zou, Y.; Andalib, M. N.; Goponenko, A.; Cheng, S. Z.; Dzenis, Y. A. Simultaneously strong and tough ultrafine continuous nanofibers. *ACS Nano* **2013,** *7* (4), 3324-3331.

(17) Ji, Y.; Li, B.; Ge, S.; Sokolov, J. C.; Rafailovich, M. H. Structure and nanomechanical characterization of electrospun PS/clay nanocomposite fibers. *Langmuir* **2006,** *22* (3), 1321-1328.

(18) Wang, W.; Barber, A. H. Measurement of size-dependent glass transition temperature in electrospun polymer fibers using AFM nanomechanical testing. *J. Polym. Sci. Pol. Phys.* **2012,** *50* (8), 546-551.

(19) Wang, W.; Barber, A. H. Diameter-dependent melting behaviour in electrospun polymer fibres. *Nanotechnology* **2010,** *21* (22), 225701.

(20) Ji, Y.; Li, C.; Wang, G.; Koo, J.; Ge, S.; Li, B.; Jiang, J.; Herzberg, B.; Klein, T.; Chen, S.; Sokolov, J. C.; Rafailovich, M. H. Confinement-induced super strong PS/MWNT composite nanofibers. *Europhys. Lett.* **2008,** *84* (5), 56002.

(21) Greenfeld, I.; Sui, X. M.; Wagner, H. D. Stiffness, Strength, and Toughness of Electrospun Nanofibers: Effect of Flow-Induced Molecular Orientation. *Macromolecules* **2016,** *49* (17), 6518-6530.

(22) Arinstein, A.; Burman, M.; Gendelman, O.; Zussman, E. Effect of supramolecular structure on polymer nanofibre elasticity. *Nat. Nanotechnol.* **2007,** *2* (1), 59-62.

(23) Guenthner, A. J.; Khombhongse, S.; Liu, W. X.; Dayal, P.; Reneker, D. H.; Kyu, T. Dynamics of hollow nanofiber formation during solidification subjected to solvent evaporation. *Macromol. Theor. Simul.* **2006,** *15* (1), 87-93.

(24) Peng, K.; Nain, A.; Mirzaeifar, R. Tracking the origins of size dependency in the mechanical properties of polymeric nanofibers at the atomistic scale. *Polymer* **2019,** *175*, 118-128.

(25) Arinstein, A. Confinement mechanism of electrospun polymer nanofiber reinforcement. *J. Polym. Sci. Pol. Phys.* **2013,** *51* (9), 756-763.

(26) Pai, C. L.; Boyce, M. C.; Rutledge, G. C. On the importance of fiber curvature to the elastic moduli of electrospun nonwoven fiber meshes. *Polymer* **2011,** *52* (26), 6126-6133.

(27) Park, J. H.; Rutledge, G. C. 50th Anniversary Perspective: Advanced Polymer Fibers: High Performance and Ultrafine. *Macromolecules* **2017,** *50* (15), 5627-5642.

(28) Kim, K. W.; Lee, K. H.; Khil, M. S.; Ho, Y. S.; Kim, H. Y. The effect of molecular weight and the linear velocity of drum surface on the properties of electrospun poly(ethylene terephthalate) nonwovens. *Fiber Polym.* **2004,** *5* (2), 122-127.

(29) Lu, J. W.; Zhang, Z. P.; Ren, X. Z.; Chen, Y. Z.; Yu, J.; Guo, Z. X. High-elongation fiber mats by electrospinning of polyoxymethylene. *Macromolecules* **2008,** *41* (11), 3762-3764.

(30) Burman, M.; Arinstein, A.; Zussman, E. Do surface effects explain the unique elasticity of polymer nanofibers? *Europhys. Lett.* **2011,** *96* (1), 16006.

(31) Park, J. H.; Rutledge, G. C. Ultrafine high performance polyethylene fibers. *J. Mater. Sci.* **2018,** *53* (4), 3049-3063.

(32) Hu, R.; Gao, E.; Xu, Z.; Liu, L.; Wang, G.; Zhu, H.; Zhang, Z. Hierarchical-structure-dependent high ductility of electrospun polyoxymethylene nanofibers. *J. Appl. Polym. Sci.* **2018,** *136* (8), 47086.

(33) Ico, G.; Showalter, A.; Bosze, W.; Gott, S. C.; Kim, B. S.; Rao, M. P.; Myung, N. V.; Nam, J. Size-dependent piezoelectric and mechanical properties of electrospun P(VDF-TrFE) nanofibers for enhanced energy harvesting. *J. Mater. Chem. A* **2016,** *4* (6), 2293-2304.

(34) Zhou, Y. X.; Freitag, M.; Hone, J.; Staii, C.; Johnson, A. T.; Pinto, N. J.; MacDiarmid, A. G. Fabrication and electrical characterization of polyaniline-based nanofibers with diameter below 30 nm. *Appl. Phys. Lett.* **2003,** *83* (18), 3800-3802.

(35) Zhong, Z.; Wingert, M. C.; Strzalka, J.; Wang, H. H.; Sun, T.; Wang, J.; Chen, R.; Jiang, Z. Structure-induced enhancement of thermal conductivities in electrospun polymer nanofibers. *Nanoscale* **2014,** *6* (14), 8283-8291.

(36) Kongkhlang, T.; Kotaki, M.; Kousaka, Y.; Umemura, T.; Nakaya, D.; Chirachanchai, S. Electrospun polyoxymethylene: Spinning conditions and its consequent nanoporous nanofiber. *Macromolecules* **2008,** *41* (13), 4746-4752.

(37) Kongkhlang, T.; Tashiro, K.; Kotaki, M.; Chirachanchai, S. Electrospinning as a new technique to control the crystal morphology and molecular orientation of polyoxymethylene nanofibers. *J. Am. Chem. Soc.* **2008,** *130* (46), 15460-15466.

(38) Ma, X. Q.; Liu, J. L.; Ni, C. Y.; Martin, D. C.; Chase, D.; Rabolt, J. F. The effect of collector gap width on the extent of molecular orientation in polymer nanofibers. *J. Polym. Sci. Pol. Phys.* **2016,** *54* (6), 617-623.

(39) Liu, Y.; Pellerin, C. Highly oriented electrospun fibers of self-assembled inclusion complexes of poly(ethylene oxide) and urea. *Macromolecules* **2006,** *39* (26), 8886-8888.

(40) Liu, Y.; Antaya, H.; Pellerin, C. Structure and phase behavior of the poly(ethylene oxide)-thiourea complex prepared by electrospinning. *J. Phys. Chem. B* **2010,** *114* (7), 2373-2378.

(41) Kakade, M. V.; Givens, S.; Gardner, K.; Lee, K. H.; Chase, D. B.; Rabolt, J. F. Electric field induced orientation of polymer chains in macroscopically aligned electrospun polymer nanofibers. *J. Am. Chem. Soc.* **2007,** *129* (10), 2777-2782.

(42) Gong, L.; Chase, D. B.; Noda, I.; Liu, J.; Martin, D. C.; Ni, C.; Rabolt, J. F. Discovery of β-Form Crystal Structure in Electrospun Poly[(R)-3-hydroxybutyrate-co-(R)-3-hydroxyhexanoate] (PHBHx) Nanofibers: From Fiber Mats to Single Fibers. *Macromolecules* **2015,** *48* (17), 6197-6205.

(43) Gong, L.; Chase, D. B.; Noda, I.; Marcott, C. A.; Liu, J.; Martin, D. C.; Ni, C.; Rabolt, J. F. Polymorphic Distribution in Individual Electrospun Poly[(R)-3-hydroxybutyrate-co-(R)-3-hydroxyhexanoate] (PHBHx) Nanofibers. *Macromolecules* **2017,** *50* (14), 5510-5517.

(44) Dazzi, A.; Prater, C. B.; Hu, Q.; Chase, D. B.; Rabolt, J. F.; Marcott, C. AFM-IR: combining atomic force microscopy and infrared spectroscopy for nanoscale chemical characterization. *Appl. Spectrosc.* **2012,** *66* (12), 1365-1384.

(45) Wang, Z.; Sun, B.; Lu, X.; Wang, C.; Su, Z. Molecular Orientation in Individual Electrospun Nanofibers Studied by Polarized AFM–IR. *Macromolecules* **2019,** *52* (24), 9639-9645.

(46) Yoshioka, T.; Dersch, R.; Greiner, A.; Tsuji, M.; Schaper, A. K. Highly Oriented Crystalline PE Nanofibrils Produced by Electric-Field-Induced Stretching of Electrospun Wet Fibers. *Macromol. Mater. Eng.* **2010,** *295* (12), 1082-1089.

(47) Dersch, R.; Liu, T. Q.; Schaper, A. K.; Greiner, A.; Wendorff, J. H. Electrospun nanofibers: Internal structure and intrinsic orientation. *J. Polym. Sci. Pol. Chem.* **2003,** *41* (4), 545-553.

(48) Cheng, Y. W.; Lu, H. A.; Wang, Y. C.; Thierry, A.; Lotz, B.; Wang, C. Syndiotactic Polystyrene Nanofibers Obtained from High-Temperature Solution Electrospinning Process. *Macromolecules* **2010,** *43* (5), 2371-2376.

(49) Richard-Lacroix, M.; Pellerin, C. Orientation and Structure of Single Electrospun Nanofibers of Poly(ethylene terephthalate) by Confocal Raman Spectroscopy. *Macromolecules* **2012,** *45* (4), 1946-1953.

(50) Richard-Lacroix, M.; Pellerin, C. Accurate New Method for Molecular Orientation Quantification Using Polarized Raman Spectroscopy. *Macromolecules* **2013,** *46* (14), 5561-5569.

(51) Richard-Lacroix, M.; Pellerin, C. Novel method for quantifying molecular orientation by polarized Raman spectroscopy: a comparative simulations study. *Appl. Spectrosc.* **2013,** *67* (4), 409-419.

(52) Richard-Lacroix, M.; Pellerin, C. Raman spectroscopy of individual poly(ethylene oxide) electrospun fibers: Effect of the collector on molecular orientation. *Vib. Spectrosc.* **2017,** *91*, 92-98.

(53) Qiu, Z. B.; Ikehara, T.; Nishi, T. Miscibility and crystallization in crystalline/crystalline blends of poly(butylene succinate)/poly(ethylene oxide). *Polymer* **2003,** *44* (9), 2799-2806.

(54) Iguchi, M. Melting and Degradation Behavior of Needle-Like Poly(Oxymethylene) Crystals. *Makromol. Chem.* **1976,** *177* (2), 549-566.

(55) Ewaldz, E.; Brettmann, B. Molecular Interactions in Electrospinning: From Polymer Mixtures to Supramolecular Assemblies. *ACS Appl. Polym. Mater.* **2019,** *1* (3), 298-308.

(56) Ding, Y. Q.; Rabolt, J. F.; Chen, Y.; Olson, K. L.; Baker, G. L. Studies of chain conformation in triblock oligomers and microblock copolymers of ethylene and ethylene oxide. *Macromolecules* **2002,** *35* (10), 3914-3920.

(57) Massa, M. V.; Dalnoki-Veress, K.; Forrest, J. A. Crystallization kinetics and crystal morphology in thin poly(ethylene oxide) films. *Eur Phys J E Soft Matter* **2003,** *11* (2), 191-198.

(58) Reneker, D. H.; Kataphinan, W.; Theron, A.; Zussman, E.; Yarin, A. L. Nanofiber garlands of polycaprolactone by electrospinning. *Polymer* **2002,** *43* (25), 6785-6794.

(59) Greenfeld, I.; Zussman, E. Polymer entanglement loss in extensional flow: Evidence from electrospun short nanofibers. *J. Polym. Sci. Pol. Phys.* **2013,** *51* (18), 1377-1391.

(60) Sun, Z. C.; Deitzel, J. M.; Knopf, J.; Chen, X.; Gillespie, J. W. The effect of solvent dielectric properties on the collection of oriented electrospun fibers. *J. Appl. Polym. Sci.* **2012,** *125* (4), 2585-2594.

(61) CRC Handbook of Chemistry and Physics. 101st ed.; Rumble, J. R., Ed. CRC Press: Boca Raton, FL: 2020.

(62) Tadokoro, H.; Kobayashi, A.; Murahashi, S.; Matsui, Y.; Kawaguchi, Y.; Sobajima, S. Normal Vibrations and Raman Spectrum of Polyoxymethylene. *J. Chem. Phys.* **1961,** *35* (1), 369-370.

(63) Linton, W. H.; Goodman, H. H. Physical properties of high molecular weight acetal resins. *J. Appl. Polym. Sci.* **1959,** *1* (2), 179-184.

(64) Kobayashi, M.; Morishita, H.; Shimomura, M.; Iguchi, M. Vibrational Spectroscopic Study on the Solid-State Phase-Transition of Poly(Oxymethylene) Single-Crystals from the Orthorhombic to the Trigonal Phase. *Macromolecules* **1987,** *20* (10), 2453-2456.

(65) Kobayashi, M.; Sakashita, M. Morphology Dependent Anomalous Frequency-Shifts of Infrared-Absorption Bands of Polymer Crystals - Interpretation in Terms of Transition Dipole Dipole Coupling Theory. *J. Chem. Phys.* **1992,** *96* (1), 748-760.

(66) Shimomura, M.; Iguchi, M.; Kobayashi, M. Vibrational Spectroscopic Study on Trigonal Polyoxymethylene and Polyoxymethylene-D2 Crystals. *Polymer* **1988,** *29* (2), 351-357.

(67) Nagai, N.; Okawara, M.; Kijima, Y. Infrared Response of Sub-Micron-Scale Structures of Polyoxymethylene: Surface Polaritons in Polymers. *Appl. Spectrosc.* **2016,** *70* (8), 1278-1291.

(68) Nagai, N.; Okada, H.; Hasegawa, T. Morphology-sensitive infrared absorption bands of polymers derived from surface polaritons. *AIP Adv.* **2019,** *9* (10), 105203.

(69) *Polymer Handbook*, Fourth ed.; John Wiley & Sons, Inc.: Hoboken, NJ: 1999.

(70) Gohil, R. M.; Patel, K. C.; Patel, R. D. Crystallization kinetics of polyacrylonitrile: single crystal growth rate and thermodynamic considerations. *Polymer* **1974,** *15* (7), 402-406.

For Table of Contents use only

Electrospinning of Highly Crystalline Polymers for Strongly Oriented Fibers

*Arnaud W. Laramée, Catherine Lanthier and Christian Pellerin**